Detection of gait from continuous inertial sensor data using harmonic frequencies

Martin Ullrich, *Student Member, IEEE*, Arne Küderle, Julius Hannink, Silvia Del Din, *Member, IEEE*, Heiko Gaßner, Franz Marxreiter, Jochen Klucken, Bjoern M. Eskofier, *Senior Member, IEEE*, and Felix Kluge

***Abstract*— Mobile gait analysis using wearable inertial measurement units (IMUs) provides valuable insights for the assessment of movement impairments in different neurological and musculoskeletal diseases, for example Parkinson's disease (PD). The increase in data volume due to arising long-term monitoring requires valid, robust and efficient analysis pipelines. In many studies an upstream detection of gait is therefore applied. However, current methods do not provide a robust way to successfully reject non-gait signals. Therefore, we developed a novel algorithm for the detection of gait from continuous inertial data of sensors worn at the feet. The algorithm is focused not only on a high sensitivity but also a high specificity for gait. Sliding windows of IMU signals recorded from the feet of PD patients were processed in the frequency domain. Gait was detected if the frequency spectrum contained specific patterns of harmonic frequencies. The approach was trained and evaluated on 150 clinical measurements containing standardized gait and cyclic movement tests. The detection reached a sensitivity of 0.98 and a specificity of 0.96 for the best sensor configuration (angular rate around the medio-lateral axis). On an independent validation data set including 203 unsupervised, semi-standardized gait tests, the algorithm achieved a sensitivity of 0.97. Our algorithm for the detection of gait from continuous IMU signals works reliably and showed promising results for the application in the context of free-living and non-standardized monitoring scenarios.**

***Index Terms*— Accelerometer, Fourier transform, Gyroscope, Parkinson's disease, Walking bouts**

This work was supported by the Bavarian Ministry for Economy, Regional Development & Energy via the Medical Valley Award 2017 (FallRiskPD Project). This project has received funding from the Innovative Medicines Initiative 2 Joint Undertaking under grant agreement No 820820. This Joint Undertaking receives support from the European Unions Horizon 2020 research and innovation programme and EFPIA.

B. M. Eskofier gratefully acknowledges the support of the German Research Foundation (DFG) within the framework of the Heisenberg professorship programme (grant number ES 434/8-1).

S. Del Din is supported by the Newcastle Biomedical Research Unit (BRU) based at Newcastle upon Tyne and Newcastle University. The work was also supported by the NIHR/Wellcome Trust Clinical Research Facility (CRF) infrastructure at Newcastle upon Tyne Hospitals NHS Foundation Trust. All opinions are those of the authors and not the funders.

M. Ullrich, A. Küderle, B. M. Eskofier, and F. Kluge are with the Machine Learning and Data Analytics Lab, Department of Computer Science, Friedrich-Alexander-Universität Erlangen-Nürnberg (FAU), Erlangen, Germany (e-mail: martin.ullrich@fau.de, arne.kuederle@fau.de, bjoern.eskofier@fau.de, felix.kluge@fau.de).

J. Hannink is with Portabiles HealthCare Technologies GmbH, Erlangen, Germany. (e-mail: julius.hannink@portabiles-hct.de).

S. Del Din is with the Institute of Neuroscience/Newcastle University Institute for Ageing, Campus for Ageing and Vitality, Newcastle University, Newcastle upon Tyne, UK (e-mail: Silvia.Del-Din@newcastle.ac.uk)

H. Gaßner, F. Marxreiter, and J. Klucken are with the Department of Molecular Neurology University Hospital Erlangen (e-mail: heiko.gassner@uk-erlangen.de, franz.marxreiter@uk-erlangen.de, jochen.klucken@uk-erlangen.de)

I. Introduction

MOBILE, sensor-based gait analysis is an applicable and objective tool for the assessment of motor impairments and disease progression in several neurological and musculoskeletal diseases, such as Alzheimer's disease [1], multiple sclerosis [2], osteoarthritis [3], or Parkinson's disease (PD) [4]. Specifically in PD, studies with inertial measurement units (IMUs) have identified a disease related reduction of gait quality, such as decreased stride length or gait speed [5] and have helped to identify characteristic motor patterns occurring prior to freezing of gait [6].

The objective information gained from sensor-based measurements has been shown to enable the prediction of conversion to PD [7] and can support clinicians in decision making during assessments in the hospital, for example for indvidualized drug treatment [8].

In recent years, the development of small and light-weight IMUs has facilitated long-term studies of gait outside of the clinical environment. Gait measurements over several days and weeks have allowed to capture a more representative disease status of patients that can for example serve the estimation of their fall risk [9], [10].

The fundamental advantage of free-living gait analysis conditions is the increase of the acquired data volume. Larger amounts of data provide a more representative impression of a patient's gait to base better treatment decisions upon. Even though long-term analysis allows to asses macro gait parameters like volume, pattern or variability of walking bouts [9], discrete spatio-temporal step characteristics, have shown to be relevant in the home-environment to reliably predict fall risk [10].

A crucial component for the computation of gait parameters is the segmentation of single strides. Several methods, like peak detection, template-matching or hidden Markov models have been proposed for this purpose [11]. Robust methods for stride segmentation which reliably reject signals of non-gait in free-living recordings can have a high computational

complexity [12]. At this point, the previously mentioned advantage of larger data volume in long-term recordings becomes a challenge.

As PD patients often spend less than ten percent of a day walking [13], [14], many gait analysis approaches detect gait prior to further processing. In their algorithm for continuous monitoring of turning movements during gait, El-Gohary et al. measured inertial sensor signals from PD patients and healthy controls at the lower back over seven days [15]. They determined walking periods by comparing the gyroscope signal norm against a predefined threshold of 15 deg/s. Periods, where this threshold was exceeded for 10 s or longer, were determined as walking bouts.

Hickey et al. extracted walking bouts and free-living steps of healthy subjects [16]. The authors applied a threshold based approach on accelerometer data measured at the lower back. Besides the high sensitivity for gait the authors reported false positives for intense cycling which resulted in similar acceleration profiles as walking.

Thresholding of the accelerometer amplitude in combination with a peak detection is the basis of the locomotion detection and cadence estimation by Paraschiv-Ionescu et al. [17]. Triaxial acceleration was measured in children with cerebral palsy and healthy controls with sensors attached to the chest and the lower back. The algorithmic pipeline included a peak enhancement, comparison of peaks against a predefined threshold for step detection, and a locomotion period detection based on the detected steps. In this approach sensitivity, specificity, and precision reached values of up to 98% for the lower back position.

Chigateri et al. recorded older adults performing scripted and unscripted tasks with a sensor attached to the lower back [18]. Their algorithm for the detection of gait and non-gait is not described in the paper. Still, the authors report an accuracy of 91.4% / 88.7% for the walking time and 97.2% / 92.2% for the non-walking time on data from scripted and unscripted activities, respectively.

In a frequency-based approach by Iluz et al., 3-d accelerometer signals from the lower back of PD patients were filtered to the locomotion frequency band of 0.5 - 3.0 Hz [19]. Local maxima resulting from a convolution with a 2 Hz sinusoidal template signal were determined as representations of gait cycles.

Another approach in the frequency domain was presented by MacDougall et al. [20]. In their study, the preferred cadence of humans during daily life locomotor activity was investigated. Analyzing the power spectra of linear acceleration measurements from different body locations revealed a dominant peak at the stride frequency of 1 Hz. Furthermore, the authors reported biomechanically induced higher frequency harmonics, which were most prominent in the signals from the lower limb sensors.

Harmonic frequency patterns during gait were exploited in the algorithm for cadence and speed estimation from wrist-worn inertial sensors by Fasel et al. [21]. The authors measured walking with healthy active persons on level and inclined terrain. They investigated the harmonic pattern in the accelerometer signal frequency domain during walking. The fundamental frequency corresponded to the stride frequency and the first harmonic to the step frequency. For the corresponding cadence estimation the approach showed an overall median relative error of -0.13%.

The literature review shows that several publications on long-term gait analysis report the usage of a gait detection as part of the analysis pipeline [15], [16], [19], [22], but only few report the performance of this specific part (e.g. [17], [18]).

Reliable detection of gait and rejection of non-gait from continuous inertial sensor measurements is crucial for efficient gait analysis. Therefore, the goal of this work was the development and evaluation of a novel algorithm for the presegmentation of gait from IMU signals. We aimed to provide a high sensitivity for gait while reliably rejecting non-gait signals at the same time. To achieve this goal, we investigated harmonic frequency patterns that typically occur in gait signals of IMUs at the feet. The foot position has been shown to yield more accurate results for the detection of gait events and the computation of temporal gait parameters compared to the lower back [23].

Training and testing of the algorithm was performed on sensor signals measured from PD patients in a clinical setting. A state-of-the-art reference method by Hickey et al. [16] was evaluated on the same data set. Additionally, we validated the proposed algorithm on unsupervised, semi-standardized gait data from patients' home environment. A preliminary version of this work has been reported in [24]. For this paper, we fundamentally improved the methodology of the algorithm, performed a cross-validation for parameter optimization and extended the evaluation data set.

Our study contributes to a more efficient processing of long-term data sets by considering only relevant signal parts in subsequent complex processing steps, such as stride segmentation and parameterization.

II. Methods

A. Data Acquisition

1) Lab data set: Two data sets were used for this study. For development and evaluation of the gait detection algorithm we used recordings from the database of the movement disorder outpatient unit of the University Hospital Erlangen. The data set contained 150 gait analysis recordings of 121 patients diagnosed with idiopathic PD (Table I).

All patients gave written informed consent and the study was approved by the local ethical committee (Re.-No. 4208). The sessions were recorded during routine patient visits in a

TABLE I: Patient characteristics.

	Lab data set	**Validation data set**
# Recordings	150	203
# Patients	121	7
Sex (m / f)	75 / 46	6 / 1
Age [years] $\pm$ SD	63.8 $\pm$ 10.6	62.5 $\pm$ 6.8
Mass [kg] $\pm$ SD	78.3 $\pm$ 17.7	80.7 $\pm$ 10.7
UPDRS-III $\pm$ SD	18.4 $\pm$ 10.0	19.0 $\pm$ 9.5
Hoehn & Yahr $\pm$ SD	2.1 $\pm$ 0.7	2.3 $\pm$ 0.8

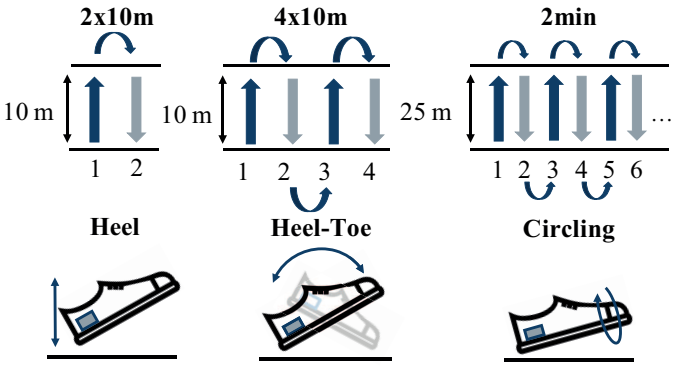

Fig. 1: Illustration of the gait and cyclic movement tests.

Fig. 2: Sensor setup for the *lab data set* (left) and *validation data set* (right), the sensors are highlighted with boxes.

supervised clinical laboratory environment, therefore this data set is called *lab data set*. In the *lab data set* the patients performed a battery of gait and movement tests.

Gait was recorded during three straight walking tests at a preferred speed (Fig. 1):

1) 2x10 m walk with a break at the turning point (*2x10m*)
2) 4x10 m walk without stops at turning points (*4x10m*)
3) 2-minute walk back and forth along a straight path of 25 m (*2min*)

Additionally, we considered three other cyclic movement tests that were performed while sitting over a period of 20 s and separately for left and right foot (Fig. 1):

1) Tapping on the ground with the heel (*heel*)
2) Tapping on the ground with heel and toes alternately (*heel-toe*)
3) Circular movement of the foot (*circling*)

Beginning and end of every test were annotated manually during the recordings. Within the *lab data set*, all 150 recordings contained the tests *2x10m*, *4x10m*, and *heel-toe*. A subset of 75 recordings additionally contained the test *2min*, the remaining 75 recordings contained the tests *heel* and *circling*. The reason for this diversity lies in changes of the test battery in the clinical routine. Both subsets are valuable for this study as the recordings with *2min* tests provide a large amount of gait data, while the other subset contributes cyclic non-gait tests for the specificity assessment.

Sensor measurements for the *lab data set* were performed using two Shimmer2R inertial sensor units [25] that were attached laterally below the ankle joint using a modified shoe (Fig. 2). The sensor units are equipped with a 3-d accelerometer (range ± 6 g) and a 3-d gyroscope (range $\pm 500°/s$) recording at a sampling-rate of 102.4 Hz.

2) Validation data set: We used an additional independent data set for the validation of the proposed algorithm (*validation data set*), which included 203 gait recordings from 7 PD patients (Table I). All patients gave written informed consent and the study was approved by the local ethical committee (Re.-No. 165_18 B). In this data set, unsupervised semi-standardized gait tests were recorded in the home environment of the patients over two weeks.

The patients were asked to perform *4x10m* gait tests three times per day (morning, noon, afternoon). They were instructed to perform the tests at preferred speed on a straight path covering a distance as close as possible to 10 m. The actual location (home, work place, outdoors,...) of the recordings could vary depending on the current location of the patient at the time of the tests.

Sensor signals for the *validation data set* were recorded with the Mobile GaitLab (Portabiles HealthCare Technologies, Erlangen, Germany). This system provides two sensors that were attached to the instep of orthopedic shoes (Fig. 2). Each sensor contains an inertial sensor unit (MPU-9250, InvenSense Inc., San Jose, CA, USA) consisting of a 3-d accelerometer (range ± 8 g) and a 3-d gyroscope (range ± 1000 $°/s$). Data were recorded at a sampling rate of 99.9 Hz and the starting and stopping of the system for the recordings was performed by the patients. Each performed gait test resulted in one sensor recording.

Prior and after the tests, the patients were standing still to allow the visual identification of the gait tests in the signals and their differentiation from any other movements that may have been recorded additionally. The exact timings of the gait tests were manually labeled by the investigators based on visual inspection of the raw data.

B. Preprocessing

All parts of the following signal processing procedures were implemented in Python, version 3.6 [26]. The entire sensor recording of each measurement session was analyzed. Raw sensor readings were calibrated to yield physically meaningful units using the method of Ferraris et al. [27]. Due to the mirrored sensor mounting on the left and right shoe, the sensor axes needed to be aligned for further processing.

For the *validation data set* the gravity direction of the sensors on the instep clip was computed to compensate for the tilt angle in the sagittal plane.

C. Gait Detection

Data from the left and right foot were analyzed individually by the algorithm, as the sensors were not synchronized. Different sensor channel configurations were considered as algorithm input:

1) acc_v : Acceleration along the vertical axis
2) acc_{norm} : Norm of the 3-d acceleration
3) gyr_{ml} : Rate of rotation around the medio-lateral axis
4) gyr_{norm} : Norm of the 3-d rate of rotation

The norm was computed as:

$$|s^{3d}| = \sqrt{s_x^2 + s_y^2 + s_z^2}, \tag{1}$$

where s^{3d} stands for 3-d accelerometer or 3-d gyroscope, respectively. The processing of the resulting 1-d time-series was

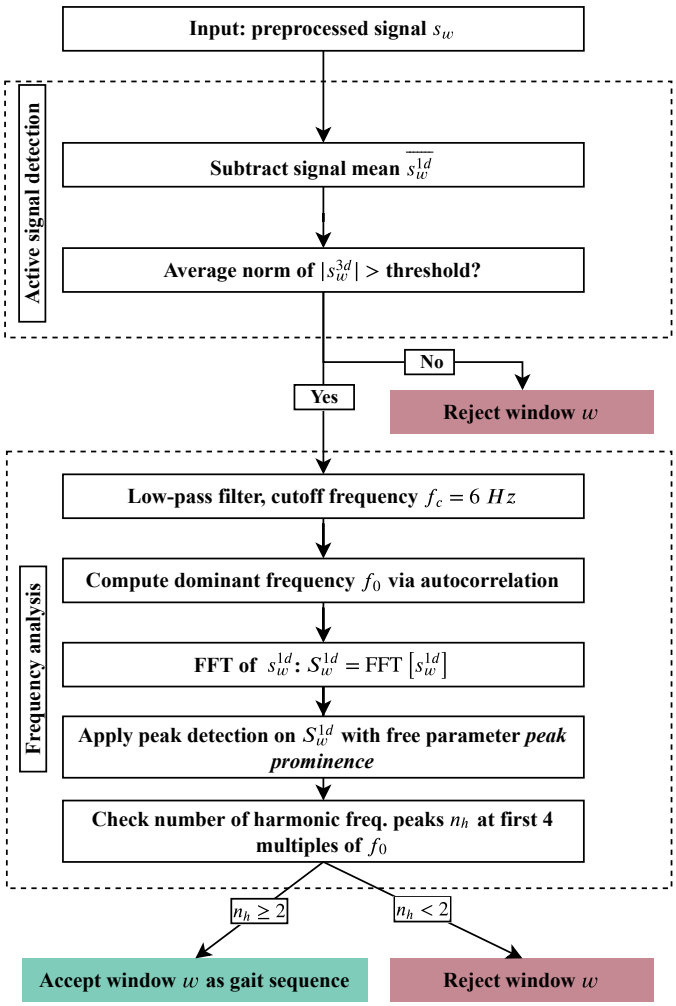

Fig. 3: Algorithm flowchart for the proposed pipeline.

similar for all sensor configurations, therefore the input signal to the algorithm is generically called s^{1d} in the following. The signal s^{1d} was analyzed in moving windows w with a length of 10 s [28], where consecutive windows overlapped by 50%. For each window w, the algorithm executed the subsequent operations (Fig. 3):

Active signal detection:

1) Subtraction of the signal mean $\overline{s_w^{1d}}$ to remove the offset.
2) Exclusion of windows that contain no activity but rest. Depending of the sensor channel configuration, resting windows were determined by comparing the average norm $\overline{s_w^{3d}}$ of the 3-d accelerometer (configurations acc_v and acc_{norm}) or the average norm of the 3-d gyroscope (configurations gyr_{ml} and gyr_{norm}) within window w against predefined thresholds [29]. For the accelerometer configurations we set this threshold to 0.2 g, for the gyroscope configurations we set it to 50 $^\circ/s$. Both thresholds were chosen in a conservative manner, based on previous experiments. A window was rejected because of resting, if the respective average norm value was below the threshold.

Frequency analysis

1) Low-pass filtering using a 4th order butterworth low-pass filter with the cut-off frequency f_c = 6 Hz. According to [20] and [24], harmonic frequencies for gait mainly appear in the low frequency range below 6 Hz.
2) Determination of the dominant frequency of the signal using autocorrelation [30].
3) Transformation of the input signal s_w^{1d} to frequency domain using fast Fourier transform (FFT):
$$S_w^{1d} = \text{FFT}\left[s_w^{1d}\right] \quad (2)$$
4) For acc_v and acc_{norm} configurations only: Multiplication of the frequency spectrum with factor 100 to work with numbers in the same order of magnitude as for gyroscope signals in subsequent steps. This multiplication was only performed for convenience reasons and does not have any functional consequences.
5) Peak detection on the frequency spectrum using the `find_peaks` function by SciPy (version 1.1.0) [31]. The *minimum peak height* was set to the mean value of the frequency spectrum below 6 Hz, to only detect peaks above the noise level. The parameter *peak prominence* was identified as a critical variable that needed to be optimized in a cross-validation (Section III-B). The *peak prominence* is a measure for the vertical distance between the peak and its lowest contour line and describes how much a peak stands out from the surrounding baseline [31].
6) Determination of the number of harmonic frequency peaks n_h at multiples of the dominant frequency with an allowed tolerance of ± 0.3 Hz. Previous work suggests the fundamental frequency for gait to be close to 1 Hz when measured at the lower limbs [5], [20], [21]. Considering the low-pass filtered signal with the 6 Hz cut-off frequency, peaks at the first four multiples of the dominant frequency were expected. Some harmonic frequency peaks may fall below the noise level, depending on the individual execution of gait [21]. Therefore, at least two out of four harmonic frequencies were required to exist in the signal in order to assign the window to be a gait sequence.

Finally, consecutive windows without breaks were concatenated to connected gait sequences. As stated in [20], gait

and cyclic non-gait movements were supposed to show a fundamental frequency of around 1 Hz (Fig. 4 and Fig. 5). We expected harmonics to appear only for gait, but non-gait signals to be almost sinusoidal.

III. Evaluation Study

A. Performance Assessment

The algorithm was evaluated regarding its sensitivity for existing gait and specificity regarding the rejection of non-gait movements.

1) Sensitivity: The ultimate goal of many gait analysis systems is the computation of spatio-temporal gait parameters. Therefore, we evaluated the sensitivity of the algorithm on the basis of single strides. Specifically we checked if the strides performed during the annotated gait tests existed in the detected gait sequences. The following pipeline was used for this purpose:

Data of the gait sequences were extracted from the continuous signal stream based on 1) the manually annotated labels and 2) the detection algorithm as described above. Single straight strides were segmented using multi-dimensional, subsequence dynamic time-warping (msDTW) [12]. The mid-stance (MS) events were detected from the segments and served as stride labels using the methods by Rampp et al. [32]. Thus, stride lists for the gait tests (= ground truth) and for the detected gait sequences (= result of the algorithm) were extracted.

Both stride lists were compared for the computation of the sensitivity or true positive rate (TPR) by counting the overall number of mutually available strides (= true positives / TP) and dividing it by the overall number of ground truth strides (= positives / P):

$$\text{sensitivity} = \text{TPR} = \frac{\text{TP}}{\text{P}} \tag{3}$$

2) Specificity: In order to evaluate the algorithm's ability to reject non-gait movements, we tested it on data from several cyclic movements described above.

Every detected gait sequence was examined regarding an overlap with any of the cyclic movement tests. The manual annotations of the movement tests served as ground truth. The false positive rate (FPR) was determined by counting the number of cyclic tests where at least one false gait sequence detection (= false positives / FP) occurred. This number was divided by the overall number of cyclic tests in the data set (= negatives / N). The specificity or true negative rate (TNR) could then be determined as

$$\text{specificity} = \text{TNR} = 1 - \text{FPR} = 1 - \left(\frac{\text{FP}}{\text{N}}\right). \tag{4}$$

Detected gait sequences that did not relate to the considered tests were ignored for the evaluation in this study.

B. Algorithm Training and Testing

The algorithm was trained and tested separately for the four different sensor channel configurations. The optimal value for the *peak prominence* parameter in the peak detection algorithm was determined in a 5-fold cross-validation with grid search. The intervals for the grid search were determined experimentally. In the cross-validation, the 150 data sets were randomly split into five subsets, where the optimal *peak prominence* per fold was determined on four subsets (120 sensor recordings) and tested on the remaining subset (30 sensor recordings). Over the five folds every subset served as the test set once. With the goal to reach both a high sensitivity and specificity for the algorithm, the Youden index was chosen as the criterion for optimal performance [33]:

$$J = \text{sensitivity} + \text{specificity} - 1 \tag{5}$$

C. Validation on Unsupervised Gait Tests

After the cross-validation and finding the optimal value for the *peak prominence* in all sensor channel configurations, the trained algorithm was applied to the independent *validation data set*. The determination of the performance followed the same steps as for the *lab data set*, however only sensitivity was computed, as none of the cyclic movement tests were performed in the *validation data set*.

D. Reference Algorithm

For the purpose of a comparison with a state-of-the art method for gait detection from continuous inertial sensor data, the walking bout detection algorithm by Hickey et al. [16] was considered. The original implementation of the algorithm was made available to the authors. The algorithm was implemented in MATLAB and executed in MATLAB version 2017b (The Mathworks, Inc., Natick, Massachusetts). The method compares the combined standard deviation of the 3-d accelerometer and the corresponding mean of the vertical acceleration against two predefined thresholds (*th-upright* and *th-still*) using windows of 0.1 s.

Areas of upright posture are detected using *th-upright* and then further characterized as dynamic and static periods using *th-still*. The predefined thresholds of the original publication were applied in this study. Additionally, *th-still* (original value: $0.05\ g$) was optimized for the sensor data collected from the foot as the dynamic range of the signal at this position is higher as for the lower back in the original publication. The tuning of the value was performed in the same grid search and cross-validation setup as described in Section III-B.

The value of *th-upright* was not adapted as the heuristic for the upright posture of the lower back can be transferred to the foot [34]. The algorithm was tested with the original and adapted threshold using the same performance criteria mentioned before.

IV. Results

After passing through the proposed algorithm, the gait sequences for the left and the right foot were available for each recording session (Fig. 6). In total, the *lab data set* contained 24218 strides in the three gait tests and 600 cyclic non-gait tests over all patients.

The optimal *peak prominence* value for each sensor channel configuration was determined based on the mean performance

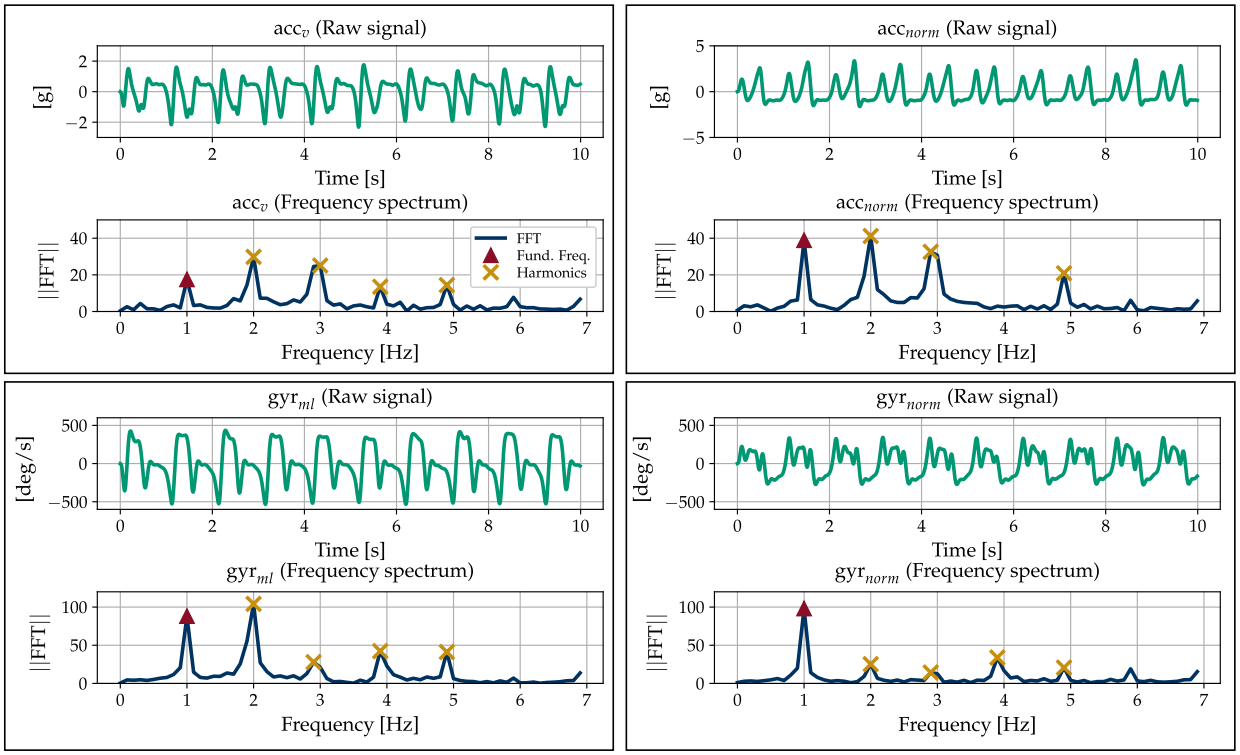

Fig. 4: Example signal window from the *2min* gait test for the four different sensor channel configurations. Every pair of subfigures shows the raw signal s_w^{1d} in the upper plot and the respective Fourier spectrum S_w^{1d} in the lower plot. The crosses indicate harmonics of the fundamental frequency (triangles) which occur during gait but are usually absent in non-gait activities.

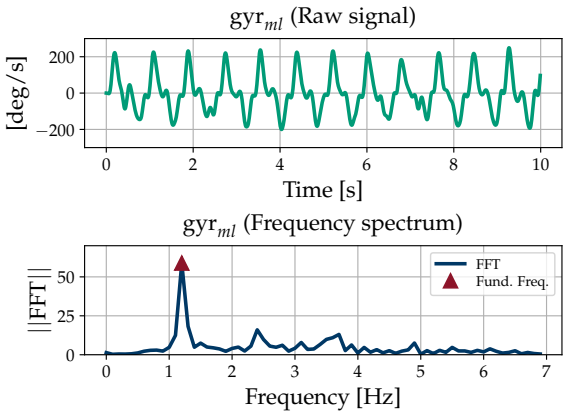

Fig. 5: Example signal window from the heel-toe test for gyr_{ml}. The triangle indicates the fundamental frequency. For non-gait usually no harmonic frequencies occur.

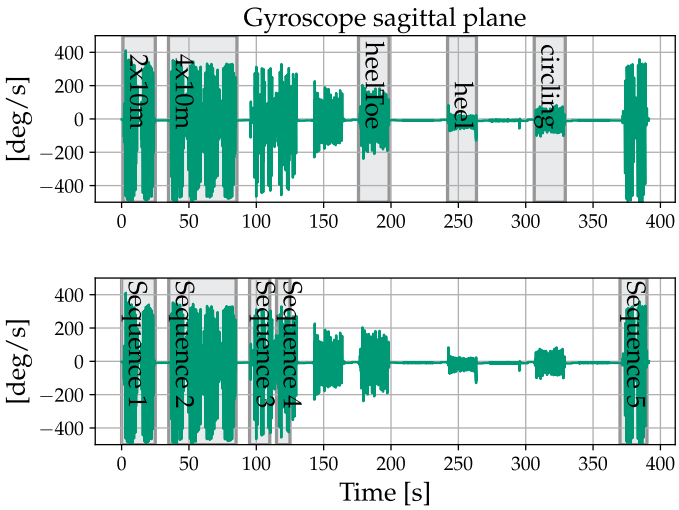

Fig. 6: Measurement session (right foot) from the *lab data set* with the manually annotated test labels (upper figure) and the result of the gait detection (lower figure). For this study only gait sequences corresponding to the tests described in Fig. 1 were considered. Potentially detected gait sequences that did not relate to the considered gait and cyclic non-gait tests (like sequences 3-5 in this figure) were ignored for the evaluation in this study.

of the algorithm on the training data in the cross-validation (Fig. 7). The best sensor channel configuration determined in the 5-fold cross-validation was gyr_{ml} (Table II). Here, the proposed gait detection reached an average sensitivity of 0.98 with a specificity of 0.96 over all folds. The best performance for gyr_{ml} with respect to the Youden index was obtained for a *peak prominence* value of 17.

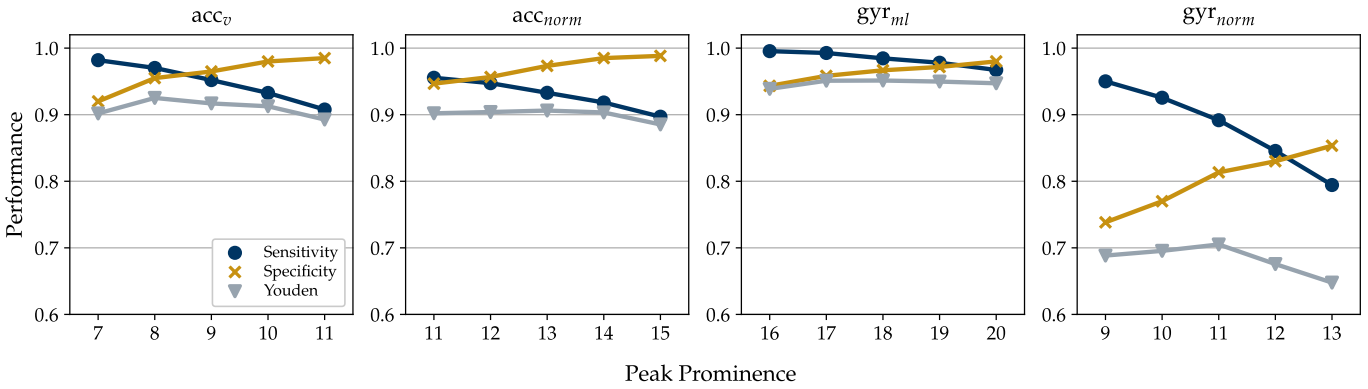

Fig. 7: Algorithm performance during training for different sensor channel configurations. In a 5-fold cross-validation the optimal value for *peak prominence* was determined in every fold's training split and then applied to the respective test split. Mean values for sensitivity (circles), specificity (crosses) and the Youden index (triangles) are shown.

TABLE II: Performance measures for the 5-fold cross-validation on the *lab data set* as mean (SD) for all sensor channel configurations (upper part) and sensitivity for the independent *validation data set* (lower part).

	acc$_v$	acc$_{norm}$	gyr$_{ml}$	gyr$_{norm}$
Lab Data Set				
Sensitivity	0.97 (0.03)	0.94 (0.04)	0.98 (0.01)	0.89 (0.04)
Specificity	0.95 (0.02)	0.96 (0.01)	0.96 (0.02)	0.81 (0.04)
Youden index	0.92 (0.02)	0.90 (0.04)	0.94 (0.01)	0.70 (0.06)
Opt. Peak Prom.	8	13	17	11
Val. Data Set				
Sensitivity	0.50	0.70	0.97	0.89

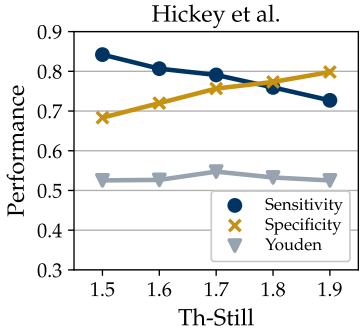

Fig. 8: Performance of the reference algorithm during training. In a 5-fold cross-validation the optimal value for *th-still* was determined in every fold's training split and then applied to the respective test split. Mean values for sensitivity (circles), specificity (crosses) and the Youden index (triangles) are shown.

In the 203 unsupervised gait tests of the *validation data set*, 9898 strides were performed in total. For the application of the proposed algorithm on the *validation data set* using the optimal values for the *peak prominence*, the configuration gyr$_{ml}$ showed the best performance with a sensitivity of 0.97 (Table II). As the *validation data set* did not contain any cyclic movement tests, only the sensitivity is reported.

The reference algorithm of Hickey et al. [16] achieved a sensitivity of 0.97 and a specificity of 0.002 on the *lab data set* in the original form. During the tuning for foot sensor position the optimal *th-still* value was determined based on the mean performance of the algorithm in the cross-validation (Fig. 8). For the optimal value of 1.7, the reference algorithm reached an average sensitivity of 0.79 (SD 0.05) with a specificity of 0.76 (SD 0.04) over all folds, resulting in an average Youden index of 0.54 (SD 0.07). On the *validation data set* the algorithm achieved a sensitivity of 0.99 with the original threshold and 0.55 with the adapted threshold.

V. Discussion

In this study, we propose an algorithm for the detection of gait from continuous inertial sensor recordings and the rejection of non-gait activities. The algorithm exploits the fact that inertial sensor signals recorded during walking result in a specific pattern of harmonic frequency peaks as previously described in the literature [20], [21].

A. Proposed Algorithm

The example plots in Fig. 4 and Fig. 5 demonstrate the discriminative power of the harmonic frequencies. A gait detection purely based on a threshold comparison of the signal or on the fundamental frequency would be prone to produce false positives. In the example signal, *heel-toe* tapping with its sinusoidal signal shape would be confounded with gait with respect to its fundamental frequency.

The cyclic movement tests available in this study are artificial tasks performed in a clinical gait assessment. Nevertheless, many activities of daily living (e.g. riding a bike) are cyclic and highly correlated with the locomotion band of 0.5 - 3 Hz [20]. The analysis of harmonics allows a reliable differentiation of gait from other non-cyclic and cyclic movements. The latter do not result in distinct frequency peaks or only one fundamental frequency peak, respectively. This needs to be verified by including more non-gait activities in future investigations.

B. Performance

One important goal of gait analysis is the estimation of spatio-temporal gait characteristics from single strides. It is

therefore necessary that an automatic detection of gait preselects the data from all strides for further analysis steps (high sensitivity).

An important additional goal of the presented approach was the rejection of signals from non-gait (high specificity). The *peak prominence* is a critical variable that directly tunes the algorithm's performance towards a higher sensitivity or specificity (Fig. 7). In all sensor channel configurations a sensitivity value of close to 1 could be reached for low *peak prominence* values. Analogously, high specificity values were achieved for higher *peak prominence* values. As a consequence of this behavior, the proposed algorithm can be seen as a threshold classifier, with the *peak prominence* as its threshold which needed to be optimized for the best performance.

In the presented evaluation study, the Youden index was utilized as a performance measure to find the optimal value for the *peak prominence*. With the Youden index we chose a performance measure that weighs the two aspects sensitivity and specificity equally and returns the optimal cutoff point with respect to both measures [33].

The best performance in the cross-validation was achieved for the gyr_{ml} configuration, followed by acc_{v}. Both of these input signals require an alignment of the sensor coordinate system with the shoe coordinate system. Contrary, the two configurations acc_{norm} and gyr_{norm} do not rely on such an alignment as the 3-d signal magnitude is independent of the sensor orientation. In applications where the alignment between the coordinate systems cannot be provided the algorithm still offers a sensitivity over 0.95 for low thresholds and for the acc_{norm} configuration also a Youden index of 0.90 at the cutoff value.

Especially the use of the accelerometer only could be of further interest, as accelerometers are less power-consuming than gyroscopes. On the one hand this could lead to an avoidance of the gyroscope for long-term studies. On the other hand it could be an option to turn on the gyroscope only, if an embedded version of the proposed algorithm based on accelerometer data detects gait in real-time.

The performance of the gyr_{norm} signal is lower than for the other three configurations. The respective signal shows a clear dominant frequency peak, but apart from that rather low harmonic peaks (Fig. 4). During the stance phase of each gait cycle the foot passes sequentially through different rotations in the single corresponding anatomical planes and the related joints [35], [36]. This sequence of rotations results in a temporal shift between characteristic signal peaks in the single 3-d gyroscope axes. Due to this shift, the signal norm becomes noisy and harmonic frequencies are attenuated.

C. Comparison to Existing Approaches

The reference algorithm by Hickey et al. [16] was tested on the *lab data set* and the *validation data set*. In our experiments the algorithm reached high sensitivities of 0.97 and 0.99 for the respective data sets with the original threshold. The results are comparable with our algorithm with the additional advantage of the high time resolution due to the small window size of 0.1 s compared to our algorithm.

The high sensitivity is, however, accompanied with a specificity of almost 0 in the *lab data set* experiments when using the original threshold. The low specificity of the reference algorithm is related to the fact that it was originally developed to work on data collected from a sensor attached to the lower back which does not measure cyclic movements of the feet.

In our experiments the general performance with respect to the Youden index could be improved by tuning the *th-still* parameter to the data from the foot-worn sensor. This reduced the sensitivity to 0.79, but increased the specificity to 0.76 for the *lab data set*. In comparison to our method, the reference algorithm still results in lower performance values even after tuning the parameter.

The approach of the method by Hickey et al. is based on comparing the mean of the vertical acceleration and the summed tri-axial standard deviation against predefined thresholds. Therefore, any movement of the sensor in upright position where the summed tri-axial standard deviation of the acceleration exceeds the *th-still* value will be detected by the algorithm and treated as gait, without further differentiation of movement patterns. For low *th-still* thresholds this results in an excellent sensitivity but very low specificity.

The locomotion detection by Paraschiv-Ionescu et al. [17] for children with cerebral palsy yielded results that are in a comparable range to our proposed method. However, it follows a different paradigm, where locomotion periods are identified after the detection of steps. That is in contrast to this approach, where walking should be detected as a pre-segmentation step in the analysis pipeline. The authors of [17] describe a sophisticated step detection algorithm, where a highly accurate locomotion detection based on the derived steps is a logical consequence.

Chigateri et al. applied a classification for walking and non-walking in their validation study on frail older people, that is not described in detail [18]. Compared to their results for the classification of walking and non-walking, our algorithm achieved a slightly higher sensitivity and comparable specificity.

D. Validation on Unsupervised Gait Tests

In order to test the transferability of our algorithm with optimized threshold values to unseen data, we performed a validation test with data from unsupervised, semi-standardized gait tests, recorded in the home environment of PD patients. The rationale of the validation test was to investigate the algorithm's performance on data from a different sensor and recording setup.

The semi-standardized gait tests were performed by the patients without any supervision. Hence, the experiments were a first step towards a validation of the algorithm on unsupervised gait. The results indicate that a transfer of the proposed algorithm to unseen data is generally possible. Especially the gyroscope configurations provided similar sensitivity values as for the *lab data set*.

The performance of the accelerometer configurations, however, dropped for the *validation data set*. Reasons for this result can be found in the different sensor positions (Fig. 2). Visual inspection of the raw signals from the two setups revealed

strong differences, especially in the acc_v signal. Different signal characteristics depending on the sensor location on the foot have previously been reported by Anwary et al. [37]. They noted that different sensor positions and orientations have a significant impact for the data collected during walking. This is also underlined by the drop of sensitivity for the reference algorithm by Hickey et al. where the adaptation of the *th-still* value obviously could not be directly transferred to the *validation data set*.

In case of our algorithm, a reliable gait detection for the sensor setup in the *validation data set* is possible using the gyroscope. Using the accelerometer only would, however, require a re-calibration of the *peak prominence*.

E. Limitations

Although we analyzed 150 clinical gait analysis sessions and 203 unsupervised and semi-standardized recordings, it cannot finally be concluded whether the results can be generalized to free-living gait. The recordings of the *lab data set* only consisted of short and standardized measurements, without influences of unpredictable activities of the daily life. The non-gait samples in the *lab data set* were limited to artificial foot movements that still provide challenging data for the algorithm, given their cyclic characteristics.

The tests on unsupervised recordings in the *validation data set* were a first step towards a validation on free-living gait, however, only with regard to the sensitivity. A proper validation would require ground truth data of whole-day recordings to assess the algorithm performance. This would also allow to get better insights into the rejection of real-world non-gait, like cycling or stair climbing.

In this study the algorithm was evaluated separately for data from the left and the right foot, resulting in individual gait sequences of the two feet. The results for both feet cannot be related as the sensors were not synchronized. Synchronization of sensors could, however, allow a more robust gait detection as the information of both sensors could be fused.

Finally, the algorithm has so far only been evaluated with data from PD patients and its applicability for other medical indications is yet to be proven. However, as long as the basic cyclic characteristics of gait are present in the signals, we expect our algorithm to work on other cohorts, too.

VI. Conclusion and Outlook

In this study, we propose a new algorithm for the detection of gait within continuous inertial sensor measurements. Our experiments have shown a reliable detection of gait and differentiation from other cyclic activities using harmonic frequencies. The algorithm reached high sensitivity and specificity values on different sensor channel configurations. Also the use of the orientation-independent sensor norm yielded high accuracy.

In future investigations, the algorithm should be validated on free-living long-term data with ground truth information about gait sequences and non-gait. For the sake of generalizability, its applicability on other clinical populations, as well as on other sensor positions and the potential gains of combining individual signal streams should be evaluated. Many previous studies used a single sensor attached to the lower back. A fair comparison with state-of-the-art algorithms for the lower back position would be desirable. This could be achieved with a data set including recordings from foot-worn and from sensors at the lower back.

The proposed algorithm is a feasible approach for the accurate detection of gait, allowing an efficient subsequent analysis of single stride gait parameters and facilitating the clinical application of mobile gait analysis in free-living conditions.

Acknowledgment

The authors would like to thank T. Reichhardt and T. Gladow for their effort in compiling the validation data set as well as all participants of the study for their contributions.

References

[1] R. Mc Ardle, R. Morris, A. Hickey, S. Del Din, I. Koychev, R. N. Gunn, J. Lawson, G. Zamboni, B. Ridha, B. J. Sahakian *et al.*, "Gait in mild alzheimers disease: Feasibility of multi-center measurement in the clinic and home with body-worn sensors: A pilot study," *J Alzheimers Dis*, vol. 63, no. 1, pp. 331–341, 2018.

[2] F. A. Storm, K. Nair, A. J. Clarke, J. M. Van der Meulen, and C. Mazza, "Free-living and laboratory gait characteristics in patients with multiple sclerosis," *PloS one*, vol. 13, no. 5, p. e0196463, 2018.

[3] S. Tadano, R. Takeda, K. Sasaki, T. Fujisawa, and H. Tohyama, "Gait characterization for osteoarthritis patients using wearable gait sensors (h-gait systems)," *J Biomechanics*, vol. 49, no. 5, pp. 684–690, 2016.

[4] A. Mirelman, P. Bonato, R. Camicioli, T. D. Ellis, N. Giladi, J. L. Hamilton, C. J. Hass, J. M. Hausdorff, E. Pelosin, and Q. J. Almeida, "Gait impairments in parkinson's disease," *Lancet Neurol*, 2019.

[5] J. C. Schlachetzki, J. Barth, F. Marxreiter, J. Gossler, Z. Kohl, S. Reinfelder, H. Gassner, K. Aminian, B. M. Eskofier, J. Winkler *et al.*, "Wearable sensors objectively measure gait parameters in parkinsons disease," *PloS one*, vol. 12, no. 10, p. e0183989, 2017.

[6] L. Palmerini, L. Rocchi, S. Mazilu, E. Gazit, J. M. Hausdorff, and L. Chiari, "Identification of characteristic motor patterns preceding freezing of gait in parkinsons disease using wearable sensors," *Front Neurol*, vol. 8, p. 394, 2017.

[7] S. Del Din, M. Elshehabi, B. Galna, M. Hobert, E. Warmerdam, U. Suenkel, K. Brockmann, F. Metzger, C. Hansen, D. Berg *et al.*, "Gait analysis with wearables predicts conversion to parkinson's disease," *Ann Neurol*, 2019.

[8] F. Marxreiter, H. Gaßner, O. Borozdina, J. Barth, Z. Kohl, J. C. Schlachetzki, C. Thun-Hohenstein, D. Volc, B. M. Eskofier, J. Winkler *et al.*, "Sensor-based gait analysis of individualized improvement during apomorphine titration in parkinsons disease," *J Neurology*, vol. 265, no. 11, pp. 2656–2665, 2018.

[9] S. Del Din, B. Galna, A. Godfrey, E. M. Bekkers, E. Pelosin, F. Nieuwhof, A. Mirelman, J. M. Hausdorff, and L. Rochester, "Analysis of free-living gait in older adults with and without parkinsons disease and with and without a history of falls: identifying generic and disease specific characteristics," *J Gerontol (Med Sci)*, 2017.

[10] A. Weiss, T. Herman, N. Giladi, and J. M. Hausdorff, "Objective assessment of fall risk in parkinson's disease using a body-fixed sensor worn for 3 days," *PloS one*, vol. 9, no. 5, p. e96675, 2014.

[11] N. Haji Ghassemi, J. Hannink, C. Martindale, H. Gaßner, M. Müller, J. Klucken, and B. Eskofier, "Segmentation of gait sequences in sensor-based movement analysis: a comparison of methods in parkinsons disease," *Sensors*, vol. 18, no. 1, p. 145, 2018.

[12] J. Barth, C. Oberndorfer, C. Pasluosta, S. Schülein, H. Gassner, S. Reinfelder, P. Kugler, D. Schuldhaus, J. Winkler, J. Klucken *et al.*, "Stride segmentation during free walk movements using multi-dimensional subsequence dynamic time warping on inertial sensor data," *Sensors*, vol. 15, no. 3, pp. 6419–6440, 2015.

[13] D. K. White, R. C. Wagenaar, T. D. Ellis, and L. Tickle-Degnen, "Changes in walking activity and endurance following rehabilitation for people with parkinson disease," *Arch Phys Med Rehab*, vol. 90, no. 1, pp. 43–50, 2009.

[14] K. Mactier, S. Lord, A. Godfrey, D. Burn, and L. Rochester, "The relationship between real world ambulatory activity and falls in incident parkinson's disease: influence of classification scheme," *Parkinsonism Relat D*, vol. 21, no. 3, pp. 236–242, 2015.

[15] M. El-Gohary, S. Pearson, J. McNames, M. Mancini, F. Horak, S. Mellone, and L. Chiari, "Continuous monitoring of turning in patients with movement disability," *Sensors*, vol. 14, no. 1, pp. 356–369, 2014.

[16] A. Hickey, S. Del Din, L. Rochester, and A. Godfrey, "Detecting free-living steps and walking bouts: validating an algorithm for macro gait analysis," *Physiol Meas*, vol. 38, no. 1, p. N1, 2016.

[17] A. Paraschiv-Ionescu, C. Newman, L. Carcreff, C. N. Gerber, S. Armand, and K. Aminian, "Locomotion and cadence detection using a single trunk-fixed accelerometer: validity for children with cerebral palsy in daily life-like conditions," *J Neuroeng Rehabil*, vol. 16, no. 1, p. 24, 2019.

[18] N. G. Chigateri, N. Kerse, L. Wheeler, B. MacDonald, and J. Klenk, "Validation of an accelerometer for measurement of activity in frail older people," *Gait Posture*, vol. 66, pp. 114–117, 2018.

[19] T. Iluz, E. Gazit, T. Herman, E. Sprecher, M. Brozgol, N. Giladi, A. Mirelman, and J. M. Hausdorff, "Automated detection of missteps during community ambulation in patients with parkinsons disease: a new approach for quantifying fall risk in the community setting," *J Neuroeng Rehabil*, vol. 11, no. 1, p. 48, 2014.

[20] H. G. MacDougall and S. T. Moore, "Marching to the beat of the same drummer: the spontaneous tempo of human locomotion," *J Appl Physiol*, vol. 99, no. 3, pp. 1164–1173, 2005.

[21] B. Fasel, C. Duc, F. Dadashi, F. Bardyn, M. Savary, P.-A. Farine, and K. Aminian, "A wrist sensor and algorithm to determine instantaneous walking cadence and speed in daily life walking," *Med Biol Eng Comput*, vol. 55, no. 10, pp. 1773–1785, 2017.

[22] A. Weiss, M. Brozgol, M. Dorfman, T. Herman, S. Shema, N. Giladi, and J. M. Hausdorff, "Does the evaluation of gait quality during daily life provide insight into fall risk? a novel approach using 3-day accelerometer recordings," *Neurorehab Neural Re*, vol. 27, no. 8, pp. 742–752, 2013.

[23] G. P. Panebianco, M. C. Bisi, R. Stagni, and S. Fantozzi, "Analysis of the performance of 17 algorithms from a systematic review: Influence of sensor position, analysed variable and computational approach in gait timing estimation from imu measurements," *Gait & posture*, vol. 66, pp. 76–82, 2018.

[24] M. Ullrich, J. Hannink, H. Gaßner, J. Klucken, B. M. Eskofier, and F. Kluge, "Unsupervised harmonic frequency-based gait sequence detection for parkinson's disease," in *2019 IEEE EMBS International Conference on Biomedical Health Informatics (BHI)*, May 2019, pp. 1–4.

[25] A. Burns, B. R. Greene, M. J. McGrath, T. J. O'Shea, B. Kuris, S. M. Ayer, F. Stroiescu, and V. Cionca, "Shimmer–a wireless sensor platform for noninvasive biomedical research," *IEEE Sens J*, vol. 10, no. 9, pp. 1527–1534, 2010.

[26] G. Van Rossum and F. L. Drake Jr, *Python tutorial*. Centrum voor Wiskunde en Informatica Amsterdam, The Netherlands, 1995.

[27] F. Ferraris, U. Grimaldi, and M. Parvis, "Procedure for effortless in-field calibration of three-axis rate gyros and accelerometers," *Sensors and Materials*, vol. 7, pp. 311–311, 1995.

[28] M. S. Orendurff, J. A. Schoen, G. C. Bernatz, A. D. Segal, and G. K. Klute, "How humans walk: bout duration, steps per bout, and rest duration." *J Rehabil Res Dev*, vol. 45, no. 7, 2008.

[29] D. M. Karantonis, M. R. Narayanan, M. Mathie, N. H. Lovell, and B. G. Celler, "Implementation of a real-time human movement classifier using a triaxial accelerometer for ambulatory monitoring," *IEEE Trans Inf Technol Biomed*, vol. 10, no. 1, pp. 156–167, 2006.

[30] R. Moe-Nilssen and J. L. Helbostad, "Estimation of gait cycle characteristics by trunk accelerometry," *J Biomechanics*, vol. 37, no. 1, pp. 121–126, 2004.

[31] E. Jones, T. Oliphant, P. Peterson *et al.* SciPy: Open source scientific tools for Python. [Online]. Available: http://www.scipy.org/

[32] A. Rampp, J. Barth, S. Schülein, K.-G. Gaßmann, J. Klucken, and B. M. Eskofier, "Inertial sensor-based stride parameter calculation from gait sequences in geriatric patients," *IEEE Trans Biomed Eng*, vol. 62, no. 4, pp. 1089–1097, 2015.

[33] R. Fluss, D. Faraggi, and B. Reiser, "Estimation of the youden index and its associated cutoff point," *Biometrical Journal: Journal of Mathematical Methods in Biosciences*, vol. 47, no. 4, pp. 458–472, 2005.

[34] G. Lyons, K. Culhane, D. Hilton, P. Grace, and D. Lyons, "A description of an accelerometer-based mobility monitoring technique," *Medical engineering & physics*, vol. 27, no. 6, pp. 497–504, 2005.

[35] M. M. Rodgers, "Dynamic biomechanics of the normal foot and ankle during walking and running," *Phys Ther*, vol. 68, no. 12, pp. 1822–1830, 1988.

[36] A. Leardini, M. G. Benedetti, L. Berti, D. Bettinelli, R. Nativo, and S. Giannini, "Rear-foot, mid-foot and fore-foot motion during the stance phase of gait," *Gait Posture*, vol. 25, no. 3, pp. 453–462, 2007.

[37] A. R. Anwary, H. Yu, and M. Vassallo, "Optimal foot location for placing wearable imu sensors and automatic feature extraction for gait analysis," *IEEE Sens J*, vol. 18, no. 6, pp. 2555–2567, 2018.